PERGAMON

Polyhedron 21 (2002) 859–865

POLYHEDRON

www.elsevier.com/locate/poly

# Spectral studies and X-ray crystal structures of three nickel(II) complexes of 2-pyridineformamide 3-piperidylthiosemicarbazone

Karen A. Ketcham [a], Isabel Garcia [b], John K. Swearingen [a], Ayman K. El-Sawaf [c], Elena Bermejo [b], Alfonso Castiñeiras [b], Douglas X. West [d,*]

[a] *Department of Chemistry, Illinois State University, Normal, IL 61790-4160, USA*
[b] *Departamento de Química Inorgánica, Universidad de Santiago de Compostela, E-15706 Santiago de Compostela, Spain*
[c] *Department of Chemistry, Faculty of Science, El Menoufia University, Shebin El-Kom, Egypt*
[d] *Department of Chemistry, 351700, University of Washington, Seattle, WA 98195-1700, USA*

Received 17 December 2000; accepted 8 January 2002

**Abstract**

Reduction of 2-cyanopyridine by sodium in dry methanol in the presence of 3-piperidylthiosemicarbazide produces 2-pyridineformamide 3-piperidylthiosemicarbazone, HAmpip. Complexes with nickel(II) have been prepared and characterized by magnetic susceptibility and spectroscopic techniques. The crystal structures of [Ni(Ampip)$_2$], [Ni(Ampip)OAc], and [Ni(HAmpip)Cl]Cl have been solved. Coordination of the anionic and neutral ligand is via the pyridyl nitrogen, imine nitrogen, and thiolato–thione sulfur. [Ni(Ampip)$_2$] is an approximately octahedral $NiN_4S_2$ center with the tridentate ligands in a meridonal arrangement. [Ni(Ampip)OAc] is essentially planar except for the acetato ligand, which is $>80^\circ$ out of the coordination plane, and the ionic [Ni(HAmpip)Cl]Cl involves the neutral thiosemicarbazone ligand. © 2002 Published by Elsevier Science Ltd.

*Keywords:* Crystal structures; 3-Piperidine; Thiosemicarbazone; 2-Pyridineformamide; Nickel(II); Spectra

## 1. Introduction

A new series of N(4)-substituted thiosemicarbazones has been prepared in which the thiosemicarbazone moiety is attached to an amide carbon rather than an aldehyde or ketone carbon in an attempt to enhance water solubility. 2-Formyl-, 2-acetyl-, and 2-benzoylpyridine N(4)-substituted thiosemicarbazones [1–3] possess substantial in vitro activity against various human tumor lines [4]. However, due to a lack of solubility in aqueous solutions, these thiosemicarbazones and their complexes show less promising in vivo activity. We have communicated our studies of metal complexes of 2-pyridineformamide thiosemicarbazone [5,6] and N(4)-methylthiosemicarbazone [7,8]. We report here spectral and structural properties of three nickel(II) complexes of 2-pyridineformamide 3-piperidylthiosemicarbazone, HAmpip, which is depicted in Fig. 1. Its structure is discussed in a communication with iron(II), cobalt(II,III), and copper(II) complexes [9].

## 2. Experimental

### 2.1. Synthetic methods

2-Cyanopyridine was purchased from Aldrich and used as received and 3-piperidylthiosemicarbazide was prepared as described by Scovill [10]. Following the literature procedure for the reduction of 2-cyanopyridine [11], sodium (0.092 g, 4 mmol) was added to 25 ml of MeOH, which had been dried over $CaSO_4$ (i.e. Drierite), and the solution stirred until complete dissolution occurred. 2-Cyanopyridine (2.6 g, 25 mmol) was then added, and the mixture stirred for 1/2 h, and 3-piperidylthiosemicarbazide (3.9 g, 25 mmol) was added in small portions over a period of 1/2 h. After addition of 15 ml of MeOH the mixture was gently refluxed for a minimum of 4 h. Slow evaporation of MeOH produced the yellow HAmpip, NMR ($CDCl_3$): N–*H* at $\delta =$

* Corresponding author. Fax: +1-206-685-8665.
*E-mail address:* westdx@chem.washington.edu (D.X. West).

0277-5387/02/$ - see front matter © 2002 Published by Elsevier Science Ltd.
PII: S0277-5387(02)00853-7

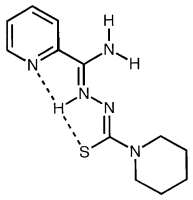

Fig. 1. Depiction of 2-pyridineformamide 3-piperidylthiosemicarbone, HAmpip.

13.186; C–*H* (Py) at $\delta = 7.995$, 7.835 and 7.422; N$H_2$ at $\delta = 6.4$ ppm; m.p., 154–156 °C.

The nickel(II) complexes were prepared as follows, nickel(II) chloride or acetate (0.002 mol) in EtOH (30 ml) was mixed with a solution of HAmpip (0.002 or 0.004 mol for [Ni(Ampip)$_2$]) in EtOH (30 ml), and the resulting mixture was stirred under reflux for 2 h or longer. The resulting solids were filtered, washed with anhydrous ether to apparent dryness, and placed on a warm plate at 35 °C until required for characterization. %Calc.(Found) for red brown [Ni(HAmpip)Cl]Cl·EtOH: C, 38.3(38.2); H, 4.8(5.3); N, 16.0(16.0); for brown [Ni(Ampip)OAc]: C, 44.3(44.3); H, 5.2(5.1); N, 18.2(18.5); for yellow brown [Ni(Ampip)$_2$]·$H_2O$: C, 48.2(47.9); H, 4.8(5.7); N, 22.9(23.3). The magnetic susceptibilities are as follows: [Ni(HAmpip)Cl]Cl·EtOH, 2.6 B.M., [Ni(Ampip)OAc], 0.0 B.M. and [Ni(Ampip)$_2$]·$H_2O$, 3.2 B.M.

### 2.2. Physical and spectroscopic methods

National Chemical Consulting, Inc. of Tenafly, NJ performed partial elemental analyses for two of the complexes and a Carlos Erba 1108 microanalyser at the Universidad de Santiago de Compostela analyzed [Ni(Ampip)OAc]. The magnetic susceptibilities were measured with a Johnson Matthey magnetic susceptibility balance. NMR spectra were obtained with a Varian 300 MHz Gemini spectrometer using $CDCl_3$ as the solvent; the chemical shifts are reported in parts per million downfield from tetramethylsilane. Infrared spectra were recorded with Nicolet 5SXC and Magna 850 FT-IR spectrometers using Nujol mulls between CsI plates; electronic spectra were acquired as Nujol mulls impregnated on filter paper with a Cary 5E spectrometer.

### 2.3. X-ray data collection, structure solution and refinement

Crystals of [Ni(HAmpip)Cl]Cl and [Ni(Ampip)$_2$] were grown from ethanol and crystals of [Ni(Ampip)OAc]

Table 1
Crystal data for [Ni(HAmpip)Cl]Cl, [Ni(Ampip)OAc], and [Ni(Ampip)$_2$]

| Compound | [Ni(HAmpip)Cl]Cl | [Ni(Ampip)OAc] | [Ni(Ampip)$_2$] |
|---|---|---|---|
| Empirical formula | $C_{12}H_{17}Cl_2N_5NiS$ | $C_{14}H_{19}N_5NiO_2S$ | $C_{24}H_{32}N_{10}NiS_2$ |
| Color; habit | brown, prism | brown, plate | brown, prism |
| Crystal size (mm) | $0.32 \times 0.08 \times 0.05$ | $0.20 \times 0.20 \times 0.05$ | $0.25 \times 0.15 \times 0.10$ |
| Crystal system | orthorhombic | triclinic | monoclinic |
| Space group | *Pbca* (# 61) | $P\bar{1}$ (#2) | $P2_1/c$ (#14) |
| Unit cell dimensions | | | |
| $a$ (Å) | 8.471(2) | 8.967(2) | 14.762(3) |
| $b$ (Å) | 21.103(6) | 9.263(3) | 13.075(4) |
| $c$ (Å) | 18.057(3) | 11.525(4) | 15.427(5) |
| $\alpha$ (°) | 90.00 | 69.07(3) | 90.00 |
| $\beta$ (°) | 90.00 | 68.37(2) | 111.71(2) |
| $\gamma$ (°) | 90.00 | 84.87(2) | 90.00 |
| Volume (Å$^3$) | 3227.9(1) | 830.3(4) | 2766.3(1) |
| $Z$ | 8 | 2 | 4 |
| Formula weight | 392.98 | 380.11 | 583.43 |
| $D_{calc}$ (Mg m$^{-3}$) | 1.617 | 1.520 | 1.401 |
| Absorption coefficient (mm$^{-1}$) | 1.662 | 1.310 | 0.886 |
| $\theta$ range for data collection (°) | 1.93–27.46 | 2.36–28.45 | 1.48–27.48 |
| Index ranges | $0 \le h \le 10$ | $-12 \le h \le 11$ | $0 \le h \le 19$ |
| | $0 \le k \le 27$ | $-12 \le k \le 0$ | $0 \le k \le 16$ |
| | $-23 \le l \le 0$ | $-15 \le l \le 14$ | $-20 \le l \le 20$ |
| Max/min transmission | 0.923/0.618 | 0.963/0.844 | 0.917/0.809 |
| Reflections collected | 3684 | 4419 | 6564 |
| Independent reflection | 2523 | 4170 | 6325 |
| Final $R$ indices [$I > 3\sigma(I)$] | $R_1 = 0.041$ $wR_2 = 0.119$ | $R_1 = 0.056$ $wR_2 = 0.105$ | $R_1 = 0.0320$ $wR_2 = 0.0789$ |
| $R$ indices (all data) | $R_1 = 0.072$ $wR_2 = 0.157$ | $R_1 = 0.071$ $wR_2 = 0.145$ | $R_1 = 0.0542$ $wR_2 = 0.0874$ |
| Goodness-of-fit | 1.049 | 0.937 | 1.025 |
| Largest difference peak and hole (e Å$^{-3}$) | 0.512 and −0.600 | 0.412 and −0.443 | 0.374 and −0.340 |

from acetonitrile, mounted on glass fibers, and used for data collection at room temperature (r.t.) with a Nonius MACH3 diffractometer, Mo Kα, $\lambda = 0.71073$ Å. A semi-empirical absorption correction, $\psi$-scan, was applied. The structures were solved by direct methods [12], which revealed the position of all non-hydrogen atoms, and refined by a full-matrix least-squares procedure using anisotropic displacement parameters [13]. The C19, C110 and C111 (and C29, C210 and C211) atoms of the piperidine rings of [Ni(Ampip)$_2$] are disordered over two positions; the occupancy factor for each was refined resulting in a value of 0.793(6) for C19A, C110A and C111A. The hydrogens attached to nitrogens were located from difference Fourier maps and refined isotropically. The remaining hydrogens were located in their calculated positions (C–H 0.93–0.97 Å) and refined using a riding model. Atomic scattering factors are from 'International Tables for Crystallography' [14] and molecular graphics are from PLATON98 [15]. Relevant crystallographic information is summarized in Table 1.

## 3. Results and discussion

The bond distances for the nickel(II) complexes are given in Table 2 and their bond angles in Table 3. Table 4 shows the mean plane data and angles between planes and Table 5 lists the hydrogen bonding interactions. Figs. 2–4 show the ORTEP drawings of [Ni(HAmpip)Cl]Cl, [Ni(Ampip)OAc], and [Ni(Ampip)$_2$], respectively.

### 3.1. Crystal structure of [Ni(HAmpip)Cl]Cl

In [Ni(HAmpip)Cl]Cl, Fig. 2, coordination of tridentate HAmpip is via the pyridyl nitrogen, imine nitrogen and thione sulfur. As is most often the case with this type of NNS tridentate ligand [16–18], the imine nitrogen coordinates with a shorter Ni–N distance than the ring nitrogen and both are shorter than the Ni–S distance, Table 2. The two *trans* angles, S1–Ni1–N11 and Cl1–Ni1–N12, are $>170°$, Table 3, the *cis* angles range from 83.49(12)° to 96.82(9)° and the N11–N12–S1–Cl1 has minimal deviation from a plane, Table 4, all of which indicate an approximately square arrangement of the four donor atoms. The thiosemicarbazone moiety is nearly co-planar with the coordinate plane.

Coordination of neutral HAmpip does not cause large changes in its bond distances since the uncoordinated HAmpip is in the bifurcated *E′* form, Fig. 1, in which the hydrogen is located on the imine nitrogen [9], the same position as nickel(II) in [Ni(Ampip)Cl]Cl. For example, the S1–C17 bond distance is unchanged and C16–N12 is 1.320(4) Å compared with 1.300(3) in HAmpip. Among the other bonds of the thiosemicarbazone moiety the largest change is exhibited by C17–N14, 1.358(3) in HAmpip to 1.320(5) Å) in [Ni(Ampip)Cl]Cl. The angle N13–C17–N14 shows the largest difference on coordination, 115.2(2)° in HAmpip and 120.0(3)° in [Ni(Ampip)Cl]Cl, but all other angles except C16–N12–N13, which is unchanged, increase or decrease by as much as 3°–4°. H13A and H15B interact with a Cl2 ion (Table 5); the two N···Cl non-bonding distances and the N–H···Cl angles are similar. The

Table 2
Selected bond distances (Å) for [Ni(HAmpip)Cl]Cl, [Ni(Ampip)(OAc)], and [Ni(Ampip)$_2$]

| Bond | [Ni(HAmpip)Cl]Cl | [Ni(Ampip)(OAc)] | [Ni(Ampip)$_2$] [a] |
|---|---|---|---|
| Ni1–S1 | 2.143(1) | 2.153 (2) | 2.4332(10) |
| | | | 2.4142(7) |
| Ni1–N11 | 1.920(3) | 1.916(4) | 2.1436(18) |
| | | | 2.1384(17) |
| Ni1–N12 | 1.845(3) | 1.829(4) | 2.0070(17) |
| | | | 2.0058(17) |
| Ni1–X [b] | 2.164(1) | 1.871(3) | |
| S1–C17 | 1.735(4) | 1.764(5) | 1.739(2) 1.755(2) |
| C16–N12 | 1.320(4) | 1.311(6) | 1.303(3) 1.306(2) |
| N12–N13 | 1.398(4) | 1.385(5) | 1.384(2) 1.383(2) |
| N13–C17 | 1.347(4) | 1.298(6) | 1.323(3) 1.323(3) |
| C17–N14 | 1.320(5) | 1.351(7) | 1.373(3) 1.366(3) |
| C16–N15 | 1.318(5) | 1.343(6) | 1.358(3) 1.345(3) |

[a] The second entries are for the S2 ligand.
[b] X = Cl1 for [Ni(HAmpip)Cl]Cl and O11 for [Ni(Ampip)OAc].

Table 3
Selected bond angles (°) for [Ni(HAmpip)Cl]Cl, [Ni(Ampip)(OAc)], and [Ni(Ampip)$_2$]

| Angle | [Ni(HAmpip)-Cl]Cl | [Ni(Ampip)-(OAc)] | [Ni(Ampip)$_2$] [a] |
|---|---|---|---|
| S1–Ni1–X [b] | 92.27(4) | 93.97(12) | 95.33(3) |
| S1–Ni1–N11 | 170.91(9) | 168.82(14) | 157.72(5) 158.35(5) |
| X [a]–Ni1–N11 | 96.82(9) | 96.75(17) | 93.47(5) 90.25(5) |
| S1–Ni1–N12 | 87.43(9) | 85.83(14) | 80.44(5) 80.50(5) |
| X [a]–Ni1–N12 | 178.2(1) | 179.36(19) | 105.52(6) 108.34(5) |
| N11–Ni1–N12 | 83.5(1) | 83.50(19) | 77.49(7) 77.89(7) |
| N11–Ni1–N21 | | | 89.05(7) |
| N11–Ni1–N22 | | | 93.27(7) |
| N12–Ni1–N21 | | | 96.03(7) |
| N12–Ni1–N22 | | | 169.13(7) |
| Ni1–S1–C17 | 98.4(1) | 95.7(2) | 94.76(7) 95.29(8) |
| Ni1–N12–C16 | 118.1(2) | 116.7(4) | 119.15(14) 117.99(13) |
| Ni1–N12–N13 | 121.1(2) | 126.1(3) | 125.71(12) 126.17(12) |
| Ni1–O11–C20 | | 121.4(3) | |
| N15–C16–N12 | 126.0(3) | 122.3(5) | 123.6(2) 123.9(2) |
| C15–C16–N12 | 111.9(3) | 114.4(5) | 115.48(17) 115.30(17) |
| C16–N12–N13 | 120.5(3) | 116.9(4) | 115.08(16) 115.09(16) |
| N12–N13–C17 | 115.3(3) | 109.9(4) | 113.30(16) 113.01(16) |
| N13–C17–N14 | 120.0(3) | 118.8(5) | 114.96(18) 116.04(18) |
| N13–C17–S1 | 117.7(3) | 122.4(4) | 125.55(15) 124.82(15) |
| N14–C17–S1 | 122.2(3) | 118.7(4) | 119.49(15) 119.14(15) |

[a] The second numbers are for the analogous angles for the S2 ligand.

Table 4
Mean planes, atoms with the largest deviations (Å) and angles (°) between planes for [Ni(HAmpip)Cl]Cl, [Ni(Ampip)(OAc)], and [Ni(Ampip)$_2$]

| Plane | RMS deviations | Largest deviations | Angle [a] |
|---|---|---|---|
| *[Ni(HAmpip)Cl]Cl* | | | |
| N11–N12–S1–Cl1 | 0.0168 | N12, 0.093(13) | |
| C16–N12–N13–C17–S1–N14 | 0.0347 | C16, 0.0501(19) | 2.77(13) |
| N11–C11–C12–C13–C14–C15 | 0.0056 | C15, 0.0084(5) | 3.75(19) |
| *[Ni(Ampip)(Oac)]* | | | |
| N11–N12–S1–O11 | 0.0336 | N12, 0.0372(21) | |
| C16–N12–N13–C17–S1–N14 | 0.0231 | C16, 0.0343(29) | 2.85(26) |
| N11–C11–C12–C13–C14–C15 | 0.0081 | N11, 0.0116(35) | 6.02(34) |
| *[Ni(Ampip)$_2$]* | | | |
| N11–N12–S1–N22 | 0.0117 | N12, 0.0140(10) | |
| C16–N12–N13–C17–S1–N14 | 0.0270 | N12, 0.0543(15) | 2.53(9) |
| N11–C11–C12–C13–C14–C15 | 0.0038 | C15, 0.0054(15) | 6.73(11) |
| N21–C21–C22–C23–C24–C25 | 0.0073 | C24, 0.0111(18) | 84.16(7) |
| C26–N22–N23–C27–S2–N24 | 0.0318 | N22, 0.0647(15) | 12.64(13) |
| N21–N22–S2–N12 | 0.0740 | N22, 0.0884(9) | 6.24(8) |

[a] Angle with previously listed plane.

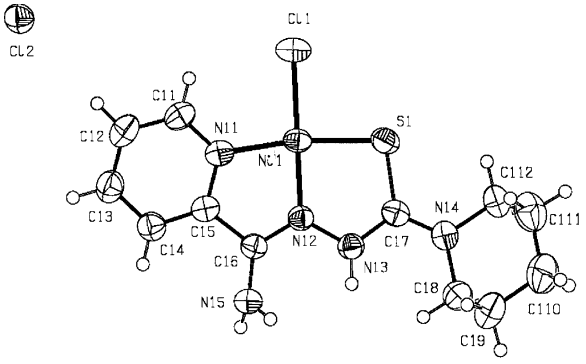


Fig. 2. ORTEP plot of [Ni(HAmpip)Cl]Cl at 50% probability.

other $NH_2$ hydrogen, H15A, hydrogen bonds to a different Cl2 ion with similar parameters to the above two interactions.

### 3.2. Crystal structure of [Ni(Ampip)OAc]

The crystal structure, Fig. 3, shows Ampip coordinated in the expected NNS tridentate fashion (i.e. the thiosemicarbazone moiety becomes conjugated) and a monodentate acetato ligand, which is the same stoichiometry found for [Ni(Am4M)OAc], where Am4M is the anion of 2-pyridineformamide N(4)-methylthiosemicarbazone [8]. The Ni1–O11 bond distance in [Ni(Ampi-

Table 5
Hydrogen bonding interactions for [Ni(HAmpip)Cl]Cl, [Ni(Ampip)(OAc)], and [Ni(Ampip)$_2$]

| D–H···A | d(D–H) (Å) | d(H···A) (Å) | d(D···A) (Å) | ∠ (DHA) (°) |
|---|---|---|---|---|
| *[Ni(HAmpip)Cl]Cl* | | | | |
| N13H13A···Cl2$^1$ | 0.94(4) | 2.30(4) | 3.243(3) | 175(3) |
| N15H15A···Cl2$^2$ | 0.84(6) | 2.39(6) | 3.217(4) | 166(5) |
| N15-H15B···Cl2$^1$ | 0.83(6) | 2.33(6) | 3.159(4) | 170(5) |
| Symmetry transformations, (1) $-x$, $y+1/2$, $-z+1/2$; (2) $x$, $-y+1/2$, $z-1/2$ | | | | |
| *[Ni(Ampip)(OAc)]* | | | | |
| N15H15A···N13 | 0.86 | 2.35 | 2.658(6) | 101.4 |
| N15H15B···O12$^1$ | 0.86 | 2.03 | 2.836(5) | 155.7 |
| Symmetry transformations, (1) $-x$, $-y$, $-z+1$ | | | | |
| *[Ni(Ampip)$_2$]* | | | | |
| N15H15A···N13 | 0.77(3) | 2.29(3) | 2.643(3) | 109(2) |
| N25H25A···N23 | 0.83(3) | 2.33(3) | 2.646(3) | 103(2) |
| N15H15B···S2$^1$ | 0.87(3) | 2.71(3) | 3.579(2) | 174(3) |
| N25H25B···S1$^2$ | 0.83(3) | 2.68(3) | 3.477(2) | 162(3) |
| Symmetry transformations,(1) $-x+1$, $-y+1$, $-z+1$; (2) $x$, $-y+1/2$, $z+1/2$ | | | | |

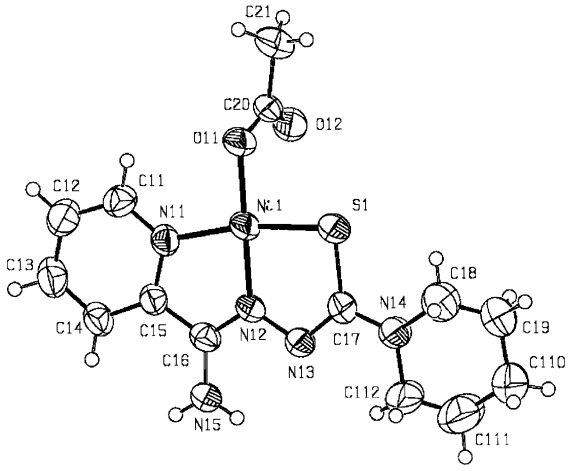


Fig. 3. ORTEP plot of [Ni(Ampip)OAc] at 50% probability.

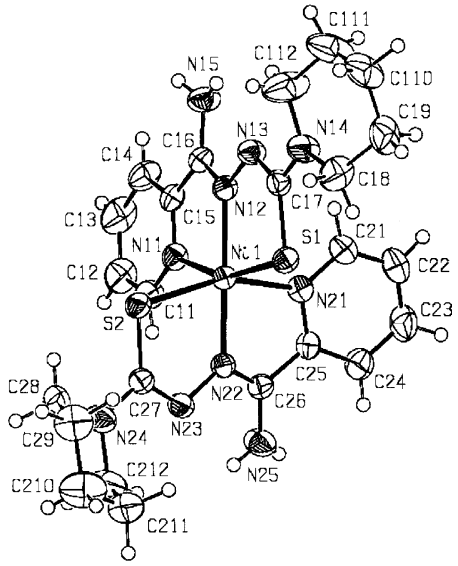


Fig. 4. ORTEP plot of [Ni(Ampip)$_2$] at 50% probability.

p)OAc], 1.871(3) Å, is marginally shorter than 1.888(3) Å for [Ni(Am4M)OAc]. The remaining metal–ligand bonds in the two complexes, as well as their thiosemicarbazone moieties, are within twice their combined e.s.d. values, and most are even more similar. Interestingly, N13–C17 is shorter than C16–N12 in [Ni(Ampip)OAc], but in [Ni(Am4M)OAc] N13–C17 is marginally longer than C16–N12. This difference is the likely cause of confusion in the thiosemicarbazone literature concerning the infrared assignment of $\nu$(C=N) in metal complexes in which a shift to both higher and lower frequencies compared with the uncomplexed thiosemicarbazone has often been reported. Since crystal structures of a number of uncomplexed thiosemicarbazones and their metal complexes have recently been reported [19], it is now known that the C16=N12 bond distance is often somewhat longer or unchanged in the complexes. This suggests that a band in the spectrum of a complex at higher energy than in the uncomplexed thiosemicarbazone is more likely due to $\nu$(N13=C17). Compared with HAmpip [9] [Ni(Ampip)OAc] has a longer S1–C17 bond, N13–C17 is $>0.040(6)$ Å shorter and C16–N12 is only marginally longer.

The anionic Ampip ligand in [Ni(Ampip)OAc] has a N11–Ni1–S1 *trans* angle of 168.82(14)° compared with 170.91(9)° for the neutral ligand in [Ni(HAmpip)Cl]Cl. The other angles about the nickel(II) ions in these complexes show smaller differences, but Ni1–S1–C17 and Ni1–N12–N13 are quite different for the two complexes, Table 2. A comparison of the neutral thiosemicarbazone ligand in [Ni(HAmpip)Cl]Cl to the anionic thiosemicarbazone ligand [Ni(Ampip)OAc] shows that the following angles C16–N12–N13, N12–N13–C17 and N13–C17–S1 are most different. The four donor atoms, N11–N12–S1–O11, in [Ni(Ampip)OAc] are nearly planar and nickel(II) is 0.0237(21) Å below the mean plane which is nearly twice the distance of 0.143(16) Å [Ni(Am4M)OAc] [8]. As is common for coordinated heterocyclic thiosemicarbazone ligands [1–3], the thiosemicarbazone moiety and pyridine ring are nearly co-planar with N11–N12–S1–O11, but the mean plane of the acetato ligand is 80.44(18)° out of the coordination plane. The distances and angles are listed in Table 5 for the hydrogen bonding interaction N15–H15A···N13, an intraligand hydrogen bond which is not found in HAmpip [9] or in complexes of HAmpip with other metal ions [9]. However, N15–H15A···N13 and the intermolecular N15–H15B···O12′ interaction are very similar to the interactions found for [Ni(Am4M)OAc] [8].

### 3.3. Crystal structure of [Ni(Ampip)$_2$]

The ORTEP plot for the approximately octahedral [Ni(Ampip)$_2$] is shown in Fig. 4. The coordination of the two ligands is meridonal due to the strong tendency toward planarity by heterocyclic thiosemicarbazones. As expected for a six-coordinate complex compared with four-coordinate complex, the donor atom bond distances to nickel(II) are all significantly longer than found for [Ni(Ampip)OAc]. The distortion from octahedral symmetry is indicated by the *trans* N11–Ni1–S1 and N21–Ni–S2 angles of approximately 158°, Table 3.

The hydrogen bonding interactions of the two ligands in [Ni(Ampip)$_2$] have similar parameters. The N15–H15B···N13 and N25–H25A···N23 intraligand interactions are identical to that discussed for [Ni(Ampip)OAc]. The other $NH_2$ hydrogen for each ligand has an intermolecular hydrogen bond to a thiolato sulfur of the other ligand on an adjacent molecule (Table 5). The mean planes of the coordinated thiosemicarbazones have small deviations from planarity although the imine nitrogens are substantially out of the plane. Table 4 shows deviations from planarity for the coordination

planes, N11–N12–S1–N22 and N21–N22–S2–N12, and for each plane the imine nitrogens, N22 and N12, respectively, show the greatest deviation from planarity.

### 3.4. Spectral and physical properties

The magnetic susceptibilities are consistent with monomeric complexes and suggest a distorted octahedral structure for [Ni(Ampip)$_2$], a planar structure for [Ni(Ampip)OAc] and a tetrahedrally distorted planar structure for [Ni(HAmpip)Cl]Cl. The latter complex could be a mixture of [Ni(HAmpip)Cl]Cl and five-coordinate [Ni(HAmpip)Cl$_2$].

The infrared bands most useful for determining the mode of coordination by HAmpip (and Ampip) are shown in Table 6. The $\nu$(C=N) band of HAmpip at 1577 cm$^{-1}$ undergoes shifts to lower frequencies in the spectra of the nickel complexes indicating coordination of the imine nitrogen [20]. A second band, assignable to $\nu$(N=C) on loss of the hydrazinic hydrogen, is often observed in the 1585 cm$^{-1}$ region of the complexes' spectra on coordination of an anionic thiosemicarbazone. Additional evidence for coordination of the imine nitrogen is the presence of $\nu$(Ni–N) bands in the 425–455 cm$^{-1}$ range [21]. The spectrum of HAmpip shows the thioamide IV band, which possesses considerable contribution from $\nu$(C–S), at 823 cm$^{-1}$, and is found at lower energy ($>60$ cm$^{-1}$) on coordination of Ampip, but to a lesser extent for [Ni(HAmpip)Cl]Cl. The $\nu$(Ni–S) bands are in the 355 cm$^{-1}$ region [22]. Coordination of the pyridyl nitrogen is indicated by a 10–24 cm$^{-1}$ shift to higher wave number for the ring in-plane deformation, $\rho$(py), which is at 594 cm$^{-1}$ in the spectrum of HAmpip. The $\nu$(M–N) bands for the pyridyl nitrogen are assigned in the 230 cm$^{-1}$ region, $\nu$(Ni–Cl) at 322 cm$^{-1}$ for [Ni(HAmpip)Cl]Cl and $\nu$(Ni–O) at 482 cm$^{-1}$ for [Ni(Ampip)OAc].

The absorption maxima of the electronic spectra of the three nickel(II) complexes and HAmpip are shown in Table 7. The higher energy $\pi\rightarrow\pi^*$ bands are omitted because their energy is unaffected by complexation. Since HAmpip is primarily the bifurcated *E′* isomer (other isomeric forms present in small amounts are *Z* and *E* with respect to the imine bond) [9], we assign the band at 32340 cm$^{-1}$ to $n\rightarrow\pi^*$ transitions for both the pyridine ring and imine function of the thiosemicarbazone moiety. The two lower energy bands result from $n\rightarrow\pi^*$ transitions associated with the thioamide portion of the thiosemicarbazone moiety. The broad band at 31 350 cm$^{-1}$ in the spectrum of [Ni(HAmpip)Cl]Cl includes the Cl$\rightarrow$Ni(II) charge transfer band [23] and the thioamide $n\rightarrow\pi^*$ intraligand bands are not shifted to as high an energy on coordination of the thione sulfur. Bands in the 20 000–23 000 cm$^{-1}$ are due to S$\rightarrow$Ni(II) charge transfer transitions and are primarily responsible for the brown color of these nickel(II) complexes. The S$\rightarrow$Ni(II) transition at 22 920 cm$^{-1}$ in the spectrum of [Ni(Ampip)$_2$] masks the $^3A_{2g}\rightarrow{}^3T_{1g}$(P) transition.

The crystal structure of [Ni(Ampip)$_2$] shows distortion from octahedral symmetry {i.e. the angle between the imine nitrogens is 169.12(7)°}. However, calculation of ligand field parameters [24] by assigning the band at 7830 cm$^{-1}$ to $^3A_{1g}\rightarrow{}^3T_{2g}$ and 11 330 cm$^{-1}$ as $^3A_{1g}\rightarrow{}^3T_{1g}$(F) yields 17 640 cm$^{-1}$ (presumably obscured by the charge transfer band at 22 920 cm$^{-1}$) for $^3A_{1g}\rightarrow{}^3T_{1g}$(P), Dq = 783 cm$^{-1}$ and B = 365 cm$^{-1}$. The Dq and B values are higher and lower, respectively, than found for bis(ligand)nickel(II) complexes prepared with 2-formylpyridine and 2-acetylpyridine thiosemicarbazones [25]. The crystal structure of [Ni(HAmpip)Cl]Cl showed it to be a nearly planar arrangement of the four donor atoms about Ni(II), Table 4. However, the NIR spectrum shows bands below 10 000 cm$^{-1}$, which are not consistent with a planar structure, and suggests that this solid is a mixture of [Ni(HAmpip)Cl]Cl and five-coordinate [Ni(HAmpip)Cl$_2$]. The number of absorption

Table 7
Solid state electronic spectra (cm$^{-1}$) for a HAmpip and its nickel(II) complexes

| Compound | Intraligand and charge transfer | d$\rightarrow$d |
|---|---|---|
| HAmpip | 32340 24360 22360 | – |
| [Ni(HAmpip)Cl]Cl | 31350 26940 25640 23560 22020 | 20380 16950 11570 6710 |
| [Ni(Ampip)(OAc)] | 31560 28570 23150 | 20833 16920 |
| [Ni(Ampip)$_2$] | 34400 29290 22920 | 11330 7830 |

Table 6
IR assignments (cm$^{-1}$) for HAmpip and its nickel(II) complexes

| Compound | $\nu$CN | $\nu$CS | $\rho$py | $\nu$MN | $\nu$MS | $\nu$MN(py) | $\nu$MX |
|---|---|---|---|---|---|---|---|
| Hampip | 1577s | 823m | 594w | – | – | – | – |
| [Ni(HAmpip)Cl]Cl | 1560m | 792m | 604w | 454w | 354m | 232m | 322m |
| [Ni(Ampip)(OAc)] [a] | 1564m | 856m | 639m | 470m | 372m | 246m | 482m |
| [Ni(Ampip)$_2$] | 1558sh | 753sh | 618w | 429m | 355m | 225m | – |

[a] Acetato ligand, $\nu_a$(COO$^-$) = 1643s, $\nu_s$(COO$^-$) = 1421m; X=O.

bands in the NIR region as well as the visible region is consistent with the presence of the latter.

The versatility of the heterocyclic thiosemicarbazones in forming a number of complexes having different coordination numbers and stereochemistry with the same metal ion has again been demonstrated. The present nickel(II) complexes involve coordination of the neutral HAmpip and anionic Ampip to produce five- and six-coordinate (and very likely five-coordinate) complexes.

## 4. Supplementary material

Crystallographic data (excluding structure factors) for the structures reported in this paper have been deposited with the Cambridge Crystallographic Data Center as CCDC-153294 for [Ni(HAmpip)Cl]Cl, CCDC-153295 for [Ni(Ampip)(OAc)] and CCDC-153296 for [Ni(Ampip)$_2$]. Copies of available material can be obtained, free of charge, on application to the Director, CCDC, 12 Union Road, Cambridge CB21EZ, UK, (fax: +44-1223-336033 or e-mail: deposit@ccdc.cam.ac.uk).

## Acknowledgements

We thank the Donors of the Petroleum Research Fund, administered by the American Chemical Society for the partial support of this research.

## References

[1] D.X. West, C.E. Ooms, J.S. Saleda, H. Gebremedhin, A.E. Liberta, Transition Met. Chem. 19 (1994) 553 and references therein.
[2] D.X. West, H. Gebremedhin, R.J. Butcher, J.P. Jasinski, A.E. Liberta, Polyhedron 12 (1993) 2489 and references therein.
[3] D.X. West, J.S. Ives, J. Krejci, M.M. Salberg, T.L. Zumbahlen, G.A. Bain, A.E. Liberta, J. Valdés-Martínez, S. Hernández-Ortega, R.A. Toscano, Polyhedron 14 (1995) 2189.
[4] (a) M.C. Miller, C.N. Stineman, J.R. Vance, D.X. West, I.H. Hall, Anticancer Res. 18 (1998) 4131;
(b) M.C. Miller, C.N. Stineman, J.R. Vance, D.X. West, I.H. Hall, Appl. Organomet. Chem. 13 (1999) 9.
[5] A. Castiñeiras, I. Garcia, E. Bermejo, D.X. West, Z. Naturforsch. Teil B 55 (2000) 511.
[6] A. Castiñeiras, I. Garcia, E. Bermejo, D.X. West, Polyhedron 19 (2000) 1873.
[7] D.X. West, J.K. Swearingen, A.K. El-Sawaf, Transition Met. Chem. 25 (2000) 87.
[8] D.X. West, J.K. Swearingen, J. Valdés-Martínez, S. Hernández-Ortega, A.K. El-Sawaf, F. van Meurs, A. Castiñeiras, I. Garcia, E. Bermejo, Polyhedron 18 (1999) 2919.
[9] K.A. Ketcham, J.K. Swearingen, A.K. El-Sawaf, A. Castiñeiras, I. Garcia, E. Bermejo, D.X. West, Polyhedron 20 (2001) 3565.
[10] J.P. Scovill, Phosphorus Sulfur Silicon Relat. Elem. 60 (1991) 15.
[11] J. van Koningsbruggen, J.G. Haasnoot, R.A.G. De Graaff, J. Reedijk, Inorg. Chim. Acta 234 (1995) 87.
[12] G.M. Sheldrick, Acta Crystallogr. A 46 (1990) 467.
[13] G.M. Sheldrick, SHELX-97. Program for the Refinement of Crystal Structures, University of Göttingen, Germany, 1997.
[14] International Tables for Crystallography, vol. C, Kluwer Academic Publishers, Dordrecht, The Netherlands, 1995.
[15] A.L. Spek, PLATON. A Multipurpose Crystallographic Tool, Utrecht University, Utrecht, The Netherlands, 1998.
[16] D.X. West, M.A. Lockwood, H. Gebremedhin, A. Castiñeiras, A.E. Liberta, Polyhedron 12 (1993) 1887.
[17] A. Castiñeiras, D.X. West, H. Gebremedhin, T.J. Romack, Inorg. Chim. Acta 216 (1994) 229.
[18] C. Maichle, A. Castiñeiras, R. Carballo, D.X. West, H. Gebremedhin, M.A. Lockwood, C.E. Ooms, T.J. Romack, Transition Met. Chem. 20 (1995) 228.
[19] (a) e.g., D.X. West, A. Castiñeiras, E. Bermejo, J. Mol. Struct. 520 (2000) 103;
(b) E. Labisbal, A. Sousa, A. Castiñeiras, J.A. García-Vázquez, J. Romero, G.A. Bain, D.X. West, Z. Naturforsch., B55 (2000) 162;
(c) D. Kovala-Demertzi, N. Kourkoumelis, M.A. Demertzis, J.R. Miller, C.S. Frampton, J.K. Swearingen, D.X. West, European J. Inorg. Chem. (2000) 727;
(d) N.T. Akinchan, U. Abram, Acta Crystallogr. C56 (2000) 549;
(e) E. Bermejo, A. Castiñeiras, R. Dominguez, R. Carballo, C. Maichle-Mössmer, J. Strähle, A.E. Liberta, D.X. West, Z. Anorg. Allg. Chem. 626 (2000) 878;
(f) G.F. de Sousa, D.X. West, C.A. Brown, J.K. Swearingen, J. Valdés-Martínez, R.A. Toscano, S. Hernández-Ortega, M. Hörner A.J. Bortoluzzi, Polyhedron 19 (2000) 841;
(g) E. Labisbal, A. Sousa, A. Castiñeiras, J.A. Garcia-Vásquez, J. Romero D.X. West, Polyhedron 19 (2000) 1255.
[20] (a) P. Sousa, J.A. Garcia-Vazquez, J.A. Masaquer, Transition Met. Chem. 9 (1984) 318;
(b) S.K. Agrawal, D.R. Tuflani, R. Gupta, S.K. Hajela, Inorg. Chim. Acta 129 (1987) 257;
(c) N. Saha, S. Sinha, Indian J. Chem. 29A (1990) 292.
[21] (a) S.K. Nag, D.S. Joarder, Can. J. Chem. 54 (1976) 2827;
(b) S.K. Sengupta, S.K. Sahni, R.N. Kapoor, Acta Chim. Acad. Sci. Hungary 104 (1990) 89;
(c) R. Roy, M. Chaudhury, S.K. Mondal, K. Nag, J. Chem. Soc., Dalton Trans., (1984) 1681;
(d) A.Z. El-Sonbati, E.M. Mabrouk, H.E. Megahed, Transition Met. Chem. 16 (1991) 280.
[22] G. DeVoto, M. Massacesi, R. Pinna, G. Ponticelli, Spectrochim. Acta, Part A 38 (1982) 725.
[23] (a) M. Suzuki, H. Kanatomi, H. Koyama, I. Murase, Bull. Chem. Soc. Japan 53 (1980) 1961;
(b) D. Kovala-Demertzi, J.M. Tsangaris, H. Hadjiliadis, Transition Met. Chem. 8 (1983) 140;
(c) M. Suzuki, H. Kanatomi, Y. Demura, I. Murase, Bull. Chem. Soc. Japan 57 (1984) 1003.
[24] A.B.P. Lever, Inorganic Electronic Spectroscopy, Elsevier, New York, 1968, p. 307.
[25] (a) D.X. West, C.S. Carlson, C.P. Galloway, A.E. Liberta, C.R. Daniel, Transition Met. Chem. 15 (1990) 91;
(b) D.X. West, C.S. Carlson, A.E. Liberta, J.N. Albert, C.R. Daniel, Transition Met. Chem. 15 (1990) 341;
(c) D.X. West, D.L. Huffman, J.S. Saleda, A.E. Liberta, Transition Met. Chem. 16 (1991) 565.